ONE-DIMENSIONAL COLLOCATION METHOD FOR THE KORTEWEG-DE VRIES EQUATION

KERREK STINSON

May 6, 2015

CONTENTS

LIST OF FIGURES

LIST OF TABLES

OVERVIEW

In this paper, we numerically model the Korteweg-de Vries equation with a one-dimensional collocation method and a finite difference scheme under a variety of conditions. To analyze the error introduced in our numerical approximation, we run our simualtion given initial conditions where the analytical solution is known.

1 KORTEWEG-DE VRIES EQUATION

The Korteweg-de Vries Equation:

$$\partial_t \phi(x,t) + \epsilon\phi(x,t)\,\partial_x \phi(x,t) + \mu\,\partial_{xxx}\phi(x,t) = 0 \tag{1}$$

$$x \in [a,b], \quad t \in [0,\infty)$$
$$\epsilon, \mu \in \mathbb{R}_+$$

Analytically, KdV is often treated on an infinite spatial domain. Imposing no boundary conditions, a solution to (1) on this domain is called a soliton, or a solitary wave. Solitons are a distinguishing feature of KdV. Despite being a nonlinear PDE, solitons display behavior that appears similar to the property of superposition for a linear PDE. It is of note that for an initial waveform with a large enough traveling velocity, KdV will eventually decompose this waveform into solitons. Looking at a variety of initial waveforms, we will see the qualitative behavior of KdV with regard to solitons.

2 NUMERICAL CONSIDERATIONS

Although, KdV is a hyperbolic PDE, we consider finite difference schemes developed for parabolic PDEs. We use these alternative methods as directly applying an implicit method to KdV leads to an equation which must be iteratively solved. However by making use of these methods, we may consider a linearly implicit method, which greatly reduces the computational difficulty. Additionally, given that we make use of the one-dimensional collocation method, the spatial domain on which we consider (1) must be finite. Throughout the paper, we enforce three boundary conditions:

$$\phi(a,t) = 0, \tag{2}$$
$$\phi(b,t) = 0, \tag{3}$$
$$\partial_x \phi(b,t) = 0. \tag{4}$$

Although these boundary conditions are not analytically true for the given initial conditions in the simulations, the true values are close enough to zero that this approximation is justified. Furthermore, for each simulation we consider a bounded time domain.

3 COLLOCATION METHOD

Given the interval $[a,b]$ we create a uniform partition of the interval, $P = \{x_1,\ldots,x_N\}$, $x_1 < x_2 < \ldots < x_N$, with $x_{k+1} - x_k = h$ for appropriate k.

In this problem, we choose to approximate our solution to KdV in S_3:

$$S_3 := \{f \in C^2[a,b] : f|_{I_k} = c_1 + c_2 x + c_3 x^2 + c_4 x^3 \ \forall k \in \{1,\dots,N-1\}\},$$

where $I_k = [x_k, x_{k+1}]$.

S_3 is finite dimensional with a basis of $N+2$ elements. We denote this basis $B = \{\nu_1,\dots,\nu_{N+2}\}$. The basis elements are the cubic B-splines, each of which spans four intervals. For a given ν_k,

$$\nu_k(x) = \begin{cases} h^{-3} g_1(x - x_{k-2}) & x \in [x_{k-2}, x_{k-1}] \\ g_2(\frac{x - x_{k-1}}{h}) & x \in [x_{k-1}, x_k] \\ g_2(\frac{x_{k+1} - x}{h}) & x \in [x_k, x_{k+1}] \\ h^{-3} g_1(x_{k+2} - x) & x \in [x_{k+1}, x_{k+2}] \\ 0 & \text{else,} \end{cases}$$

where $g_1(x) = x^3$ and $g_2(x) = 1 + 3x + 3x^2 - 3x^3$. To define the basis functions, we extend P uniformly three steps on either side: $P_{ext} = \{x_{-2}, x_{-1}, x_0, x_1, \dots, x_N, x_{N+1}, x_{N+2}, x_{N+3}\}$, where $x_{N+1} = x_N + h$ and the others are defined similarly. Letting P_{ext} define the nodal points, $B = \{\nu_k|_{[a,b]} : k = 0,\dots,N+1\}$.

We approximate the solution to KdV with

$$\Phi = \sum_{i=0}^{N+1} \alpha_i(t)\nu_i(x).$$

Thus we see the approximation will be an element of S_3 for fixed t.

We construct Φ such that it satisfies the PDE at the midpoints of each I_k:

$$\partial_t \Phi(x_{k+1/2}, t) + \Phi(x_{k+1/2}, t)\, \partial_x \Phi(x_{k+1/2}, t) + \partial_x^3 \Phi(x_{k+1/2}, t) = 0 \quad \forall k \in \{1,\dots,N-1\}$$

This defines a system of $N-1$ ODEs. In combination with the prescribed boundary conditions, (2) - (4), we have $N+2$ equations defining the system of $N+2$ unknowns.

Using our defintion of Φ, we may more explicitly write this system as follows:

$$V\alpha' + (V\alpha) *_C (V_x\alpha) + V_{xxx}\alpha = 0,$$

$$(C_1 + C_2 + C_3)\alpha = 0$$

where $*_C$ represents component wise multiplication of vectors.

$$V = \begin{bmatrix} v_1(x_{1+1/2}) & \dots & v_{N+2}(x_{1+1/2}) \\ \vdots & \ddots & \vdots \\ v_1(x_{N-1/2}) & \dots & v_{N+2}(x_{N-1/2}) \\ 0 & \dots & 0 \\ \vdots & \ddots & \vdots \\ 0 & \dots & 0 \end{bmatrix}$$

$$V_x = \epsilon \begin{bmatrix} v_1'(x_{1+1/2}) & \dots & v_{N+2}'(x_{1+1/2}) \\ \vdots & \ddots & \vdots \\ v_1'(x_{N-1/2}) & \dots & v_{N+2}'(x_{N-1/2}) \\ 0 & \dots & 0 \\ \vdots & \ddots & \vdots \\ 0 & \dots & 0 \end{bmatrix}$$

$$V_{xxx} = \mu \begin{bmatrix} v_1'''(x_{1+1/2}) & \dots & v_{N+2}'''(x_{1+1/2}) \\ \vdots & \ddots & \vdots \\ v_1'''(x_{N-1/2}) & \dots & v_{N+2}'''(x_{N-1/2}) \\ 0 & \dots & 0 \\ \vdots & \ddots & \vdots \\ 0 & \dots & 0 \end{bmatrix}$$

$$C_1 = \begin{bmatrix} 1 & 4 & 1 & 0 & \dots & 0 \\ 0 & 0 & 0 & 0 & \ddots & \vdots \\ \vdots & \ddots & \ddots & \ddots & \ddots & \vdots \\ 0 & \dots & \dots & \dots & \dots & 0 \end{bmatrix}$$

$$C_2 = \begin{bmatrix} 0 & \dots & \dots & \dots & \dots & 0 \\ \vdots & \ddots & \ddots & \ddots & \ddots & \vdots \\ 0 & \ddots & 0 & 0 & 0 & 0 \\ 0 & \ddots & 0 & 1 & 4 & 1 \\ 0 & \dots & 0 & 0 & 0 & 0 \end{bmatrix}$$

$$C_3 = \begin{bmatrix} 0 & \dots & \dots & \dots & \dots & 0 \\ \vdots & \ddots & \ddots & \ddots & \ddots & \vdots \\ 0 & \ddots & 0 & 0 & 0 & 0 \\ 0 & \dots & 0 & -3/h & 0 & 3/h \end{bmatrix},$$

where each matrix is $N+2 \times N+2$, each of the V matrices represent the points evaluated in the intervals I_k, and the matrices C_1, C_2, and C_3 represent the boundary conditions (2) - (4) respectively.

Note that $(V\alpha) *_C (V_x\alpha) = ((V\alpha) *_C V_x)\alpha$ if we allow $*_C$ to represent row wise multiplication on V_x by the corresponding scalar in the preceeding vector.

4 METHODS FOR TIME STEPPING

We consider modifications of both backwards Euler and Crank-Nicolson.

Consider our time interval, $[0, T]$. Let us make a uniform partion: $P_t = \{t_0, \ldots, t_m\}$, $t_{k+1} - t_k = r$ for appropriate k and $r = T/m$.

To allow explicit comparison with KdV, (1), we let $\Phi^n = V\alpha^n$, $D_x\Phi^n = V_x\alpha^n$, and $D_x^3\Phi^n = M\alpha^n$ where $M = V_{xxx} + C_1 + C_2 + C_3$. We include our boundary conditions in this term as it allows for the most succinct representation, while still conveying the same information.

4.1 Linearly Extrapolated Backward Euler

For KdV, applying Backwards Euler in time, our implicit approximation is given by

$$\frac{\Phi^{n+1} - \Phi^n}{r} + \Phi^{n+1} D_x(\Phi^{n+1}) + D_x^3(\Phi^{n+1}) = 0$$

Using extrapolation, we contruct our new method, the linearly extrapolated backward Euler (BELE):

$$\frac{\Phi^{n+1} - \Phi^n}{r} + \Phi^{n} D_x(\Phi^{n+1}) + D_x^3(\Phi^{n+1}) = 0$$

Writing this in terms of α, we have

$$\frac{V\alpha^{n+1} - V\alpha^n}{r} + (V\alpha^n) *_C (V_x\alpha^{n+1}) + M\alpha^{n+1} = 0$$

Thus,

$$(V\alpha^{n+1} + r(V\alpha^n) *_C V_x + rM)\alpha^{n+1} = V\alpha^n,$$

and we see that BELE is linearly implicit.

To implement BELE, we must find the initial condition for α given $g(x) = \phi(x, 0)$. To do this we solve the following equation for α^0:

$$(V + C_1 + C_2 + C_3)\alpha^0 = G, \tag{5}$$

where

$$G = \begin{bmatrix} g(x_{1+1/2}) & \ldots & g(x_{N-1/2}) & 0 & 0 & 0 \end{bmatrix}^T,$$

This system constructs α^0 such that it satisfies our initial condition at the midpoints of I_k and the three boundary conditions. This choice is congruent with the collocation method. For further work on BELE, see Schatz [1, p. 199]. We will also discuss the method further in Section 6.

4.2 Linearly Extrapolated Crank-Nicolson

We derive the extrapolated method from the approximation:

$$\frac{\alpha^{n+1} - \alpha^n}{r} = F\Big(\frac{\alpha^{n+1} + \alpha^n}{2}\Big), \tag{6}$$

As F is Lipschitz, it is straightforward to show that this method is convergent with $O(r^2)$.

Equation (6) is equivalent to

$$\frac{\Phi^{n+1}-\Phi^n}{r}+\Big(\frac{\Phi^{n+1}+\Phi^n}{2}\Big)D_x\Big(\frac{\Phi^{n+1}+\Phi^n}{2}\Big)+D_x^3\Big(\frac{\Phi^{n+1}+\Phi^n}{2}\Big)=0. \tag{7}$$

To implement (7) we must solve a nonlinear system at each timestep; this is a result of the term $\Phi^{n+1}D_x(\Phi^{n+1})$. To avoid this, we use the linearly extrapolated Crank-Nicolson method (CNLE):

$$\frac{\Phi^{n+1}-\Phi^n}{r}+\Big(\widehat{\Phi}^n\Big)D_x\Big(\frac{\Phi^{n+1}+\Phi^n}{2}\Big)+D_x^3\Big(\frac{\Phi^{n+1}+\Phi^n}{2}\Big)=0, \tag{8}$$

$$\widehat{\Phi}^n=\frac{3}{2}\Phi^n-\frac{1}{2}\Phi^{n-1}$$

$\widehat{\Phi}^n$ was chosen as such because $\frac{3}{2}\phi(t_n)-\frac{1}{2}\phi(t_{n-1})=(\phi(t_{n+1})+\phi(t_n))/2+O(r^2)$, which is found by expanding Taylor Series.

Putting (8) in terms of α:

$$V\Big(\frac{\alpha^{n+1}-\alpha^n}{r}\Big)+\widehat{\alpha}^n *_C V_x\Big(\frac{\alpha^{n+1}+\alpha^n}{2}\Big)+M\Big(\frac{\alpha^{n+1}+\alpha^n}{2}\Big)=0,$$

$$\widehat{\alpha}^n=V\Big(\frac{3}{2}\alpha^n-\frac{1}{2}\alpha^{n-1}\Big)$$

Rearranging,

$$\Big(V+\frac{r}{2}\widehat{\alpha}^n *_C V_x+\frac{r}{2}M\Big)\alpha^{n+1}=\Big(V-\frac{r}{2}\widehat{\alpha}^n *_C V_x-\frac{r}{2}M\Big)\alpha^n.$$

Once again, we have obtained a linearly implicit method. However, this is a multistep method, and to begin use CNLE, we must have both α_0 and α_1. We compute α_0 as in (5) and use a predictor corrector method to compute α_1.

Predictor-corrector method:

$$V\Big(\frac{\alpha^{1,0}-\alpha^0}{r}\Big)+V\alpha^0 *_C V_x\Big(\frac{\alpha^{1,0}+\alpha^0}{2}\Big)+M\Big(\frac{\alpha^{1,0}+\alpha^0}{2}\Big)=0,$$
$$V\Big(\frac{\alpha^1-\alpha^0}{r}\Big)+V\Big(\frac{\alpha^1+\alpha^0}{2}\Big) *_C V_x\Big(\frac{\alpha^1+\alpha^0}{2}\Big)+M\Big(\frac{\alpha^1+\alpha^0}{2}\Big)=0.$$

We consider in further detail CNLE in Section 6. For further reading on CNLE and the predictor-corrector method, we recommend the reader to Schatz [1, p. 204].

5 SIMULATIONS

All simulations in this section use CNLE. The primary focus of the simulations is to assess whether the numerical model appropriately describes the qualitative behavior of KdV.

5.1 Maxwellian Initial Condition

See Figures 1 and 2.

The Maxwellian initial condition simply refers to a Gaussian distribution at $t = 0$.

Initial Condition:

$$\phi(x, 0) = e^{-x^2}$$

We consider $t \in [0, 12.5]$ and $x \in [-15, 15]$, and run the simulation for two values of μ while fixing $\epsilon = 1$. We set $h = 0.1$ and $r = 0.01$. Note the behavior as μ decreases. The shallow ripples move towards soliton waveforms as μ decreases. This is a characteristic behavior of the Maxwellian initial condition. For further information on the Maxwellian initial condition we direct the reader to Canivar [2].

5.2 Soliton

See Figure 3.

We consider one soliton with initial condition

$$\phi(x, 0) = 3c \ \mathrm{sech}^2(ax - 6).$$

Parameters:

$$c = .3$$
$$\epsilon = 1$$
$$\mu = 5 \times 10^{-4}$$
$$a = \frac{1}{2}\sqrt{\epsilon c/\mu}$$

For the soliton, we consider $t \in [0, 3]$ and $x \in [0, 2]$. We set both h and r to 0.01. The simulation displays the expected behavior of the soliton. The numerical approximation maintains its waveform and velocity as it travels. For further references on the topic of solitons, we direct the reader to Brauer [3] and Canivar [2].

5.3 First Wave Interaction

See Figure 4.

We use the prescribed initial condition

$$\phi(x, 0) = 12\frac{3 + 4\cosh(2x) + \cosh(4k)}{(3\cosh(k) + \cosh(3k))^2}.$$

Parameters:

$$\epsilon = 6$$
$$\mu = 1$$

For the first wave interaction, we consider $t \in [0, 0.3]$ and $x \in [-5, 15]$. We choose $h = 0.1$ and $r = 0.01$.

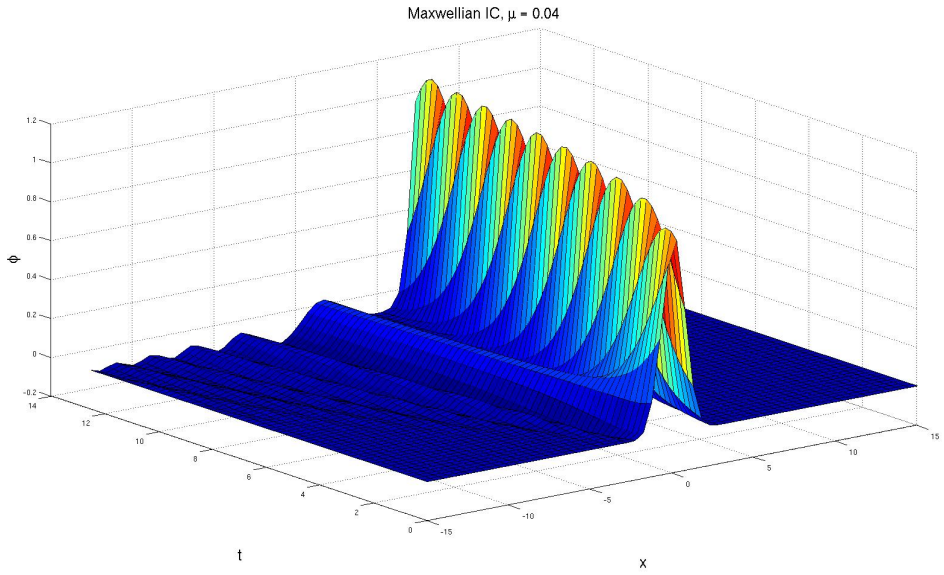

Figure 1: Maxwellian IC with $\mu = 0.04$

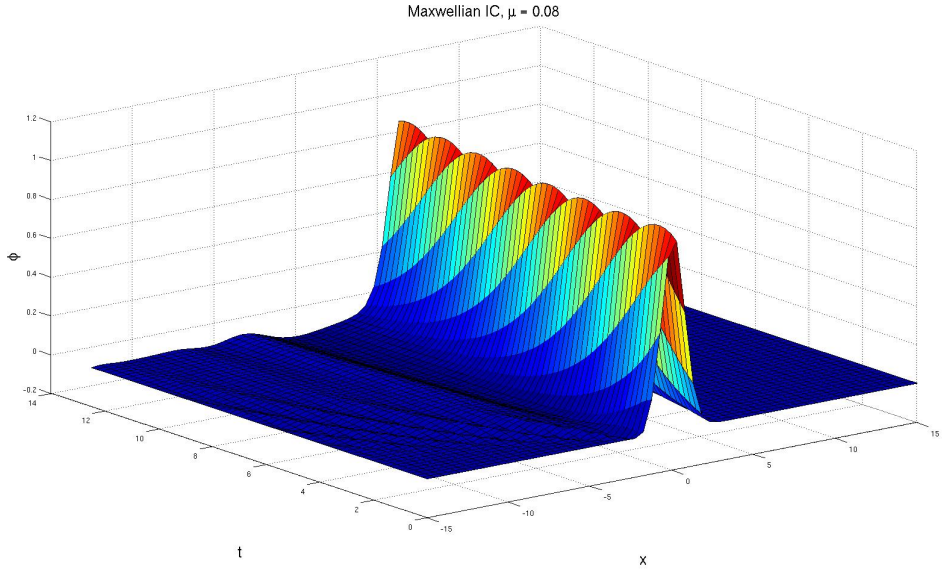

Figure 2: Maxwellian IC with $\mu = 0.08$

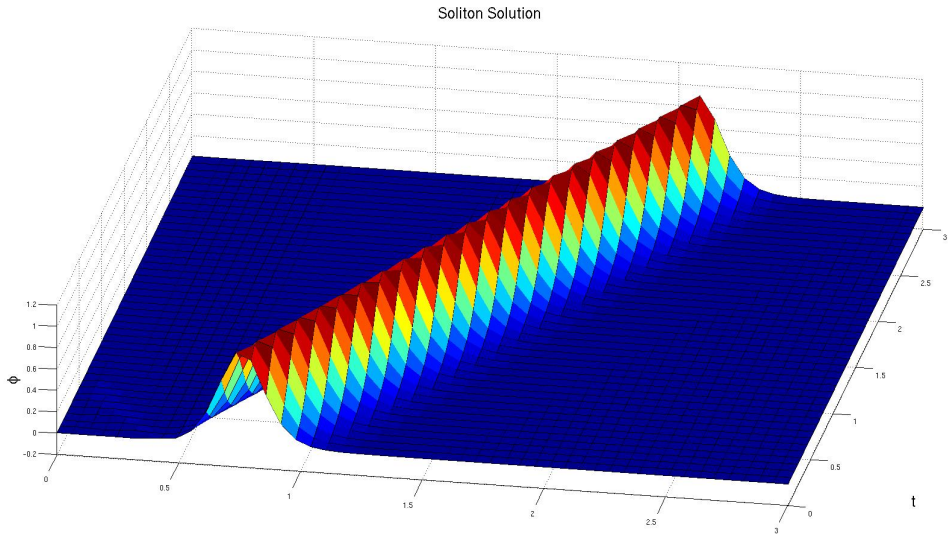

Figure 3: Soliton

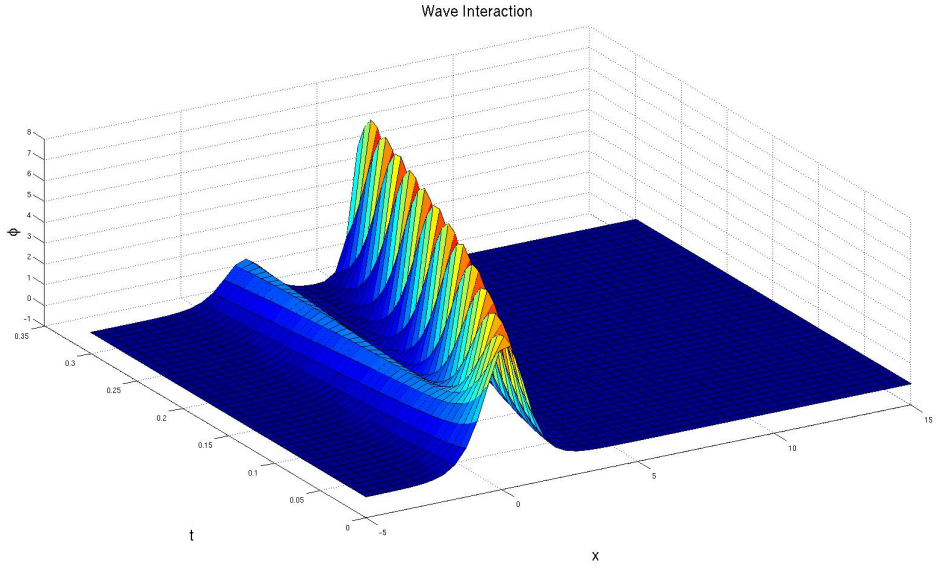

Figure 4: First Wave Interaction

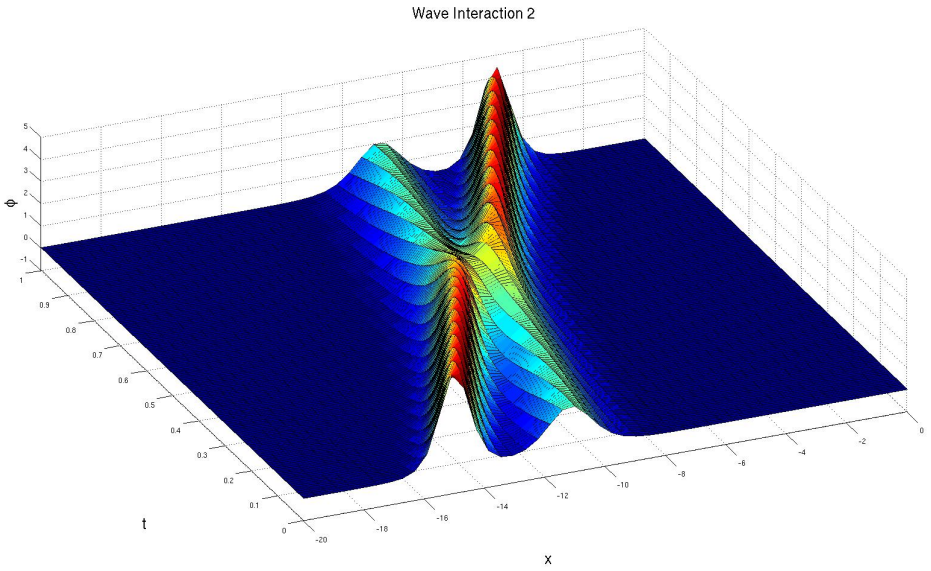

Figure 5: Second Wave Interaction

5.4 Second Wave Interaction

See Figure 5.

The intitial condition:

$$\phi(x,0) = 5\frac{4.5(\mathrm{csch}(1.5(k+14.5)))^2 + 2(\mathrm{sech}(k+12))^2}{(3\coth(1.5(k+14.5)) - 2\tanh(k+12))^2}.$$

Parameters:

$\epsilon = 6$

$\mu = 1$

For the second wave interaction, we consider $t \in [0,1]$ and $x \in [-20,0]$. We choose $h = 0.1$ and $r = 0.01$.

Comparing our results for the First and Second Wave interaction to those in Dehghan [4], we see that our model correctly captures the behavior of KdV in regards to wave motion. Most notably in the second wave interaction, although the waves intersect, and do affect each other's path, intensity is not lost in the waveforms after passing. This exemplifies the idea of soliton superposition in KdV.

6 NUMERICAL ERROR ANALYSIS FOR THE 2-D METHOD

We note that further analysis should be performed on the one-dimensional Collocation method; however, this report focuses on the integrated collocation method and finite difference scheme.

To perform the analysis, we consider the simulation for the soliton. This allows us to compare the numerical approximation generated by the method with the analytic solution at a given time. We analyze both the BELE and CNLE methods and use both the ∞-norm and 2-norm in the analysis.

6.1 BELE

For the soliton, we consider the same parameters as in Section 5. We choose h, the spatial step, and set $r = h^2$.

We find the absolute error of the numerical approximation with respect to the analytic solution,

$$\phi(x, 0) = 3c \operatorname{sech}^2(ax - aect - 6). \tag{9}$$

The data is presented in Table 1.

Table 1: Errors for Soliton, BELE

	Norm	
$j,\ h = (1/2)^j$	$\|E\|_\infty$	$\|E\|_2$
4	2.014159	8.696917
5	0.346916	1.554004
6	0.108652	0.479781
7	0.028750	0.126591
8	0.007296	0.032077

We fit a line of best fit to the plot of $\log(h)$ vs. $\log(\|E\|)$. For the ∞ and 2-norm we have a lines with slope 1.9811 and 1.9783 respectively.

In Schatz [1, p. 199], BELE is considered for parabolic FEM Galerkin method. For a given time that is included in our partition of the temporal interval, it is found that

$$\|\Phi^n - \phi(\cdot, t_n)\| = O(\|\Phi^0 - \phi(\cdot, 0)\| + h^2 + r)$$

for some $C > 0$. Given that $r = h^2$,

$$\|\Phi^n - \phi(\cdot, t_n)\| = O(\|\Phi^0 - \phi(\cdot, 0)\| + h^2)$$

Furthermore, from convergence tests on the time independent collocation method, we expect $\|\Phi^0 - \phi(\cdot, 0)\| = O(h^2)$. Thus, under the given conditions we expect

$$\|\Phi^n - \phi(\cdot, t_n)\| = O(h^2).$$

This is precisely what the errors show with comparison to the line of best fit, which has slope ≈ 2, indicating second order convergence.

6.2 CNLE

Once again, we consider the same parameters as in Section 5. We choose h, the spatial step, and set $r = h$.

We find the absolute error of the numerical approximation with respect to the analytic solution (9).

We fit a line of best fit to the plot of $\log(h)$ vs. $\log(\|E\|)$. For the ∞ and 2-norm we have a lines with slope 1.3554 and 1.2566 respectively.

In Schatz [1, p. 204], CNLE is considered for parabolic FEM Galerkin method. For a given time that is included in our partition of the temporal interval, it is found that

$$\|\Phi^n - \phi(\cdot, t_n)\| = O(\|\Phi^0 - \phi(\cdot, 0)\| + h^2 + r^2)$$

Table 2: Errors for Soliton, CNLE

	Norm	
$j,\ h = (1/2)^j$	∞	2
6	0.081917	0.384133
7	0.030287	0.141727
8	0.012900	0.060480
9	0.005964	0.027979

for some $C > 0$. Given that $r = h$,

$$\|\Phi^n - \phi(\cdot, t_n)\| = O(\|\Phi^0 - \phi(\cdot, 0)\| + h^2)$$

Furthermore, from convergence tests on the time independent collocation method, we expect $\|\Phi^0 - \phi(\cdot, 0)\| = O(h^2)$. Thus, we expect

$$\|\Phi^n - \phi(\cdot, t_n)\| = O(h^2).$$

Given our lines of best fit, we see that the data for error does not agree with the expected order of convergence. Given that our approximation behaved as expected for BELE, we imagine this error was introduced in the implementation of CNLE, perhaps the predictor-corrector method. Lastly, it is possible that this bound for convergence does not hold for KdV. This will demand further attention in a later report.

7 RESULTS AND DISCUSSION

Through numerous qualititative examples, it was found that this model does capture the behavior of KdV's waveforms. Furthermore, using a the linearly implicit BELE, we numerically found convergence rates similar to rates for FEM Galerkin for parabolic PDEs. This numerical result indicates that it will be worth exploring the theoretical convergence of BELE for KDV. Somewhat surprisingly, CNLE's convergence was not comparable to the theoretical convergence rates for FEM Galerkin for parabolic PDEs. This too indicates that further work should be done with the method. However, in contrast to BELE, more numerical computations should be ran before venturing into theoretical territory.

Extending the error analysis done in this paper, more initial conditions for which the analytic solution is known should be simulated. For computational feasibility, these analytic solutions should be found on spatial domains similar to that of the soliton explored in this paper. This is in contrast to the wave interaction simulations, which have analytic solutions, but on too large of a domain for finding convergence rates in a reasonable amount of time.

Once an appropriately accurate time-stepping method has been implemented, such as a second order method, higher order collocation should be explored. This means the next step is correcting the current implementation of CNLE or adopting a new method.

REFERENCES

[1] Alfred Schatz, Vidar Thomée, Wolfgang Wendland *Mathematical Theory of Finite and Boundary Element Methods*, DMV Seminar, Band 15, Birkhauser Verlag, Boston, Massachusetts, 1990.

[2] Aynur Canivar, Murat Sari, Idris Dag *A Taylor-Galerkin finite element method for the KdV equation using cubic B-splines* , Elsevier, Online, 2010.

[3] Klaus Brauer *The Korteweg-de Vries Equation: History, exact Solutions, and graphical Representation* , University of Osnabruck, Germany, 2000.

[4] Mehdi Dehghan, Ali Shokri *A numerical Method for KdV Equation using collocation and radial basis functions* , Springer Science, Online, 2006.